Chapter 7

Mathematical calculations for aerosol microphysics studies

In this chapter we present the mathematical detail required to develop the experimental method used to separate nucleation, condensation, and coagulation processes, as described in section 6.2. We also develop criteria for validating the simplified coagulation model appearing in that section.

7.1 Homogeneous nucleation as a source of critical cluster nucleii

As the sulfuric acid vapor is entrained into the flowtube, the supersaturation increases dramatically with the decreasing temperature. Density fluctuations within the gas are thus increasingly likely to lead to clusters of molecules for which the surface vapor pressure is less than or equal to the surrounding gas. The Kelvin effect has a tendency to cause such clusters to evaporate quickly as the vapor pressure above the surface of small particles is significantly higher than the equilibrium pressure above a flat surface. Assuming macroscopic quantities such as the surface tension are meaningful at molecular length scales, thermodynamics describes the critical cluster size required to be stable (with respect to evaporation) at a given supersaturation. Since the Kelvin effect decreases as the particle size increases, the stable cluster size can be defined as a function of the supersaturation, and as expected the stable cluster size decreases with increasing supersaturation (see fig. 7-1). The rate at which these particles form however is outside the realm of thermodynamics. Despite a formal nucleation rate theory dating back to

1926, homogeneous nucleation remains an active field of research with widely discrepant experimental results, especially regarding its temperature variation.[1] Here we present a model of the nucleation process present at early stages of the particle formation process. This will offer insight into the evolving distribution of critical nuclei, providing the seed distribution for our coagulation studies.

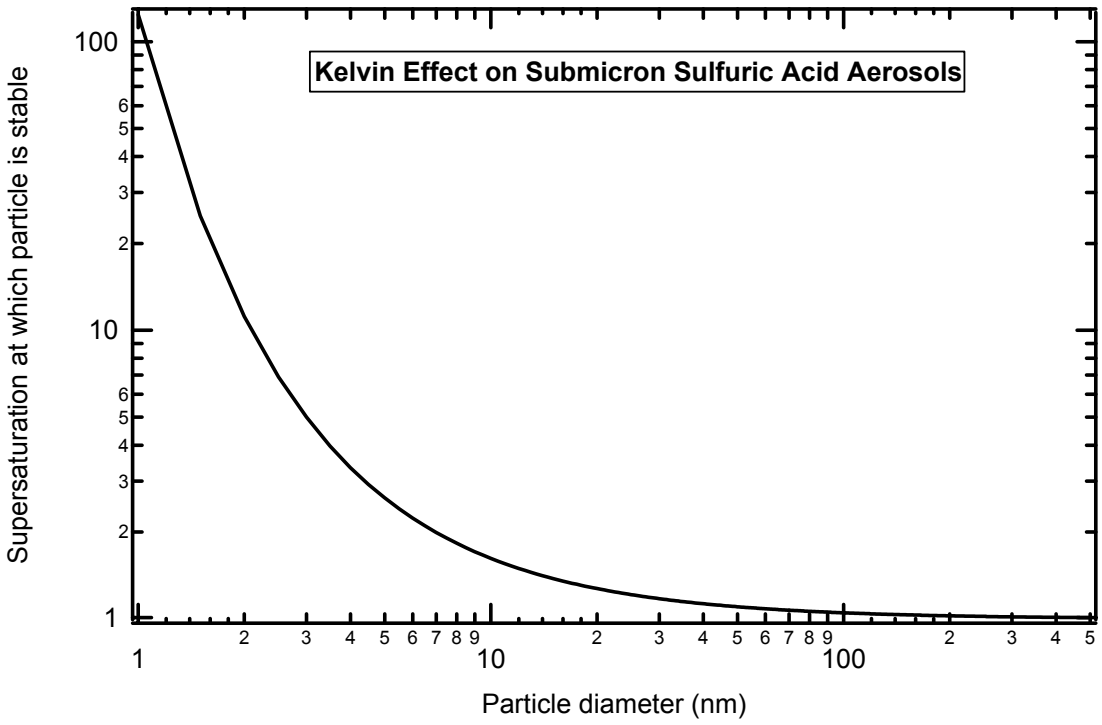

Figure 7-1: The Kelvin effect links the particle size to the ratio of the partial pressure above the particle surface to that above a flat surface. This defines the supersaturation at which a given particle size is stable (neither evaporating nor growing).

The nucleation rate function describes how quickly critical clusters of a given size appear. This enables us to define a function of the following form:

$$\begin{aligned} J_{nuc} &= f(C_m, T, S) \quad v = v_{crit}(S,T) \\ J_{nuc} &= 0 \qquad\qquad\quad v \neq v_{crit} \end{aligned} \tag{7.1}$$

Here, C_m is the monomer (gas phase) concentration, S is the supersaturation, T is the temperature, and v_{crit} is the volume of a critical cluster, defined by the thermodynamics as mentioned above. Since the supersaturation is increasing with time, different sized monomers will appear at different times in the flowtube. Those appearing at earlier times at different rates will persist, and we thus will have a distribution of sizes forming. This distribution of critical cluster sizes will largely depend on the change in supersaturation with time. We describe the dynamics of the size distribution, dN/dv through the following:

$$\frac{d}{dt}\left(\frac{dN}{dv}\right) = J_{nuc}(C_m, T, S)\delta(v - v_{crit}(S,T)) \qquad (7.2)$$

The δ function on the right hand side delivers a spike centered on v_{crit} whose area is unity with units nm^{-3}, such that the overall units are m^{-3} s^{-1} nm^{-3}. The expression describes how fast particles of a given size are appearing. Numerical results for conditions similar to those in these flowtube studies are shown in fig. 7-2. In this particular system the partial differential equation shown in eq. 7.2 is simpler than it may appear. The particles formed at time $t + dt$ simply add to those formed at t, independent of the shape of the distribution at t. This contrasts to growth dynamics where the distribution at $t + dt$ depends both on flowtube conditions and the shape of the distribution at t.

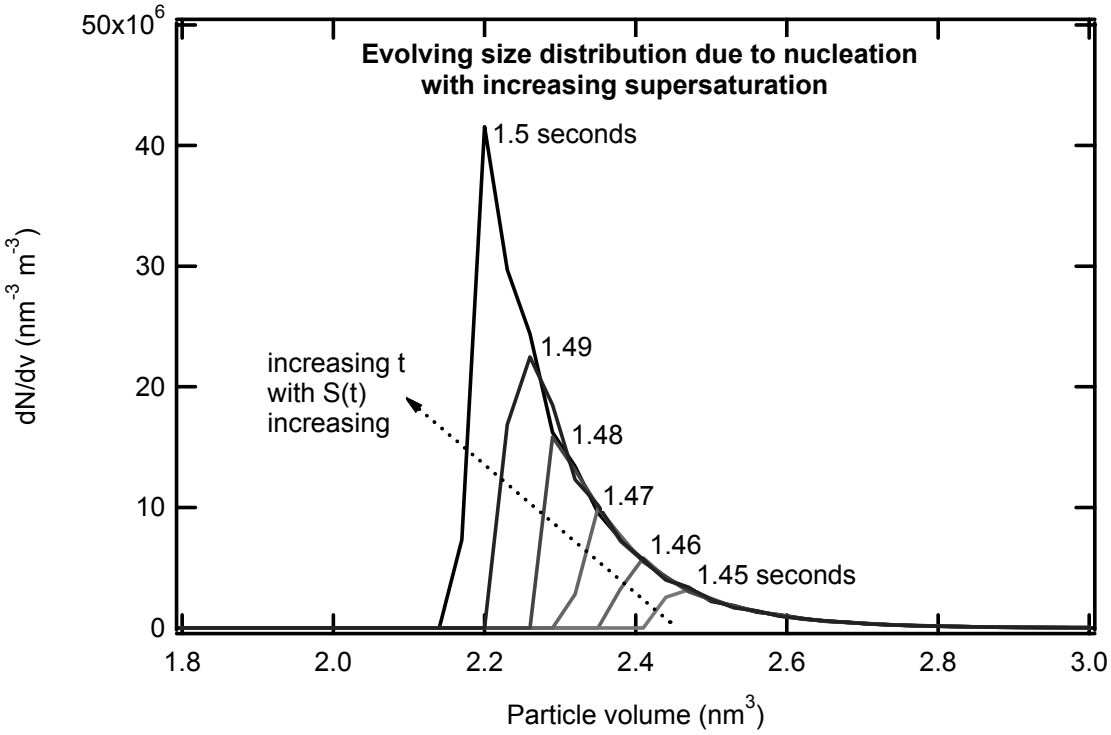

Figure 7-2: Evolving distribution of critical clusters under conditions of increasing supersaturation.

Since the supersaturation is increasing with time, smaller nuclei become stable and form at higher rates, so the distribution grows leftward as shown. In our system, growth on such small particles is very rapid (despite the Kelvin effect) and the supersaturation is driven very rapidly to 1 as we show below.

7.2 Modeling particle growth in flowtube studies

Once the supersaturation is greater than some critical value, S_{crit}, homogeneous nucleation produces critical clusters at rates in excess of 10^3 cm^{-3} s^{-1} (see fig. 6-7). These clusters, initially at very high S begin to collect vapor through condensation, in turn reducing S very rapidly such

that the nucleation rate is dramatically decreased. Due to the fast condensation on critical clusters, the nucleation rate in our experiments rises and falls very quickly. Such a nucleation "burst" delivers an initial number of critical clusters that grow and coagulate before they are sampled into the AMS. In this section we present the physics of particle growth on submicron particles.

In the absence of chemical reactions, particle size change is driven by the gas phase concentration gradient prevailing at the particle surface. In the case of particles whose radii are small enough that fluxes can be considered kinetic ($Kn >> 1$, $a << 300$ nm), the net flux of molecules to the surface is given by (molecules m^{-2} s^{-1}):

$$J = \frac{(n_\infty - n_a)\bar{c}}{4} = \frac{\alpha(P_\infty - P_s)}{\sqrt{2\pi m_1 K_B T}} \tag{7.3}$$

Here, m_1 is the mass of a single molecule. The vapor pressures just above the particle surface and far from it are denoted by P_a and P_∞ respectively. Formulations for the dynamics of size distributions of particles undergoing condensation or evaporation can be found in the literature. Analytical solutions are available only for the simplest cases. Here we present a simplified model for the case of a discrete aerosol size.

The change in the number of molecules composing the particle is given by:

$$\dot{N}_p = \frac{dN_p}{dt} = \pi D_p{}^2 J \tag{7.4}$$

while the change in mass is

$$\dot{m}_p = m_1 \pi D_p{}^2 J \tag{7.5}$$

At any moment in time the particle mass is given by:

$$m_p(t) = \rho \frac{\pi D_p(t)^3}{6} \tag{7.6}$$

Using the method described in sec. 3.2, the rate of size change can be found through the transformation:

$$\dot{D}_p = \frac{dD_p}{dt} = \frac{dm}{dt}\frac{dD_p}{dm} = \frac{2m_1 J}{\rho} \tag{7.7}$$

Since our particles begin as critical clusters with volumes on the order of 1 nm^3, the vapor pressure above their surface will be enhanced by the Kelvin effect. We must therefore write the pressure above the surface of the particle as:

$$P_s = P^0 Exp(\frac{4\sigma v_1}{K_B T D_p}) \tag{7.8}$$

Here P^0 is the pressure at equilibrium above a flat surface, σ is the surface tension, and v_1 is the volume of a single molecule of the substance. We can estimate the importance of this quantity by setting the argument in the exponent to 0.1 and solving for the diameter, to find that for $D_p <$ 25 nm the pressure at the surface deviates significantly from its equilibrium value (see fig. 7-1). In the model we develop here however, we can show that this effect does not significantly change the growth rate of particles since for very small sizes the supersaturation drives the condensation more than the Kelvin effect resists it.

Since there is loss of gas-phase species, this must be coupled into the process. The rate of change of gas-phase concentration due to condensation on particles (again assumed monodisperse) is given by:

$$\dot{n} = -\pi D_p{}^2 J N_0 \tag{7.9}$$

Here N_o is the number of particles per m^3 of air.

We may now bring *n(t)* naturally into the condensing flux with:

$$J(n,T,D_p) = \frac{\alpha}{\sqrt{2\pi m_1 K_B T}}[n(t)K_B T - P^0(T)Exp(\frac{4\sigma v_1}{K_B T D_p(t)})] \tag{7.10}$$

We therefore have the following system of coupled ordinary differential equations to be solved simultaneously for the change in concentration and particle size in time:

$$\dot{D}_p = \frac{2m_1 J(n(t), T(t), D_p(t))}{\rho} \tag{7.11}$$

$$\dot{n} = -\pi D_p(t)^2 J(n(t), T(t), D_p(t)) N_0$$

The initial conditions are defined by *n(0)* for the initial gas-phase concentration and $D_p(0)$ for the critical cluster size. No known analytical solution exists for this system, but a numerical solution is straightforward, using either Euler or Runge-Kutta integration (see fig. 7-3). This model confirms that particle nucleation under conditions present in this study leads to very rapid growth of particles and consequent decrease of gas phase density, such that nucleation and growth can be effectively removed from the general dynamic equation and we can focus our attention on coagulation alone.

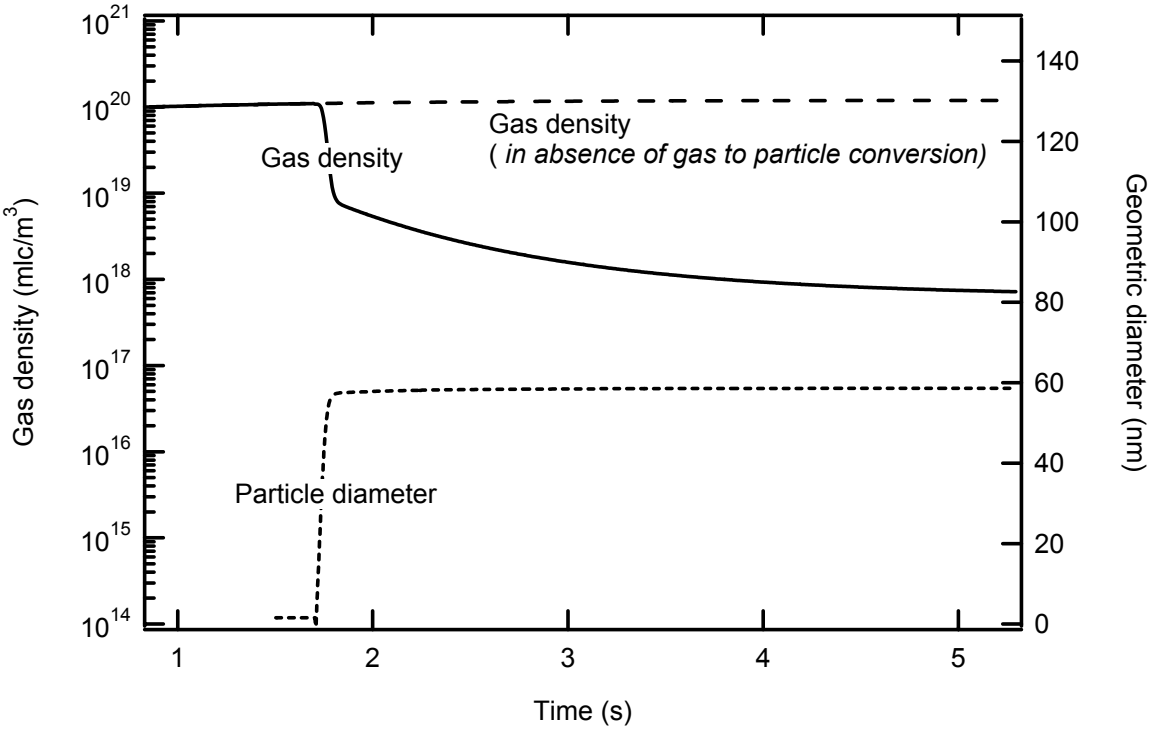

Figure 7-3: Rapid condensation on particles delivers an initial number density of particles which continue to grow slightly until detection, maintaining S=1 in the cooling carrier flow.

Effect of condensation on polydisperse distributions

The above model describes particle growth due to condensation assuming a single particle size (the size distribution is a delta function). Here, we will discuss qualitatively what effect condensation will have on a polydisperse size distribution with time.

Eq. 7.3 shows the flux onto a particle surface in the case of kinetic mass transport. This is only valid in the limit where the particle radius is much less than the mean free path of the air molecules surrounding the particle (Kn >>1). Since the condensing gas phase flux is independent of size, it follows that all aerosol sizes will encounter the same growth rate (see eq. 7.7). Such condensation conditions would lead to a simple rightward shift of the entire size distribution through diameter space in time. At the other extreme (Kn << 1), the flux of condensing gas phase species to the aerosol surface can be shown[2] to go as the inverse of the

particle radius. In such a case, eq. 7.7 indicates that the growth rate is larger for smaller particles. Distributions of particles condensing in this fashion would exhibit a faster rightward shift of the left side of the size distribution than the right side, such that the distribution is increasingly monodisperse.

Determining coagulation time with incomplete saturation

In these experiments the sulfuric acid vapor is entrained by flowing N_2 over a sulfuric acid reservoir at a known temperature. In systems where use of a frit is not possible due to complications arising from formation of particles from popping bubbles, the partial pressure at the reservoir exit is not likely to obtain its equilibrium value. The extent of equilibration can be approximated experimentally if there are no wall losses by comparing the mass in the observed particles to the expected amount if all the gas at equilibrium vapor pressure were to condense (see fig. 6-8). We define the equilibration extent, ε as the ratio of the actual to the equilibrium vapor pressure:

$$\varepsilon \equiv \frac{p_0}{p^o(T_{res})} \tag{7.12}$$

The concentration of sulfuric acid exiting the reservoir is therefore given by:

$$C_0 = \frac{\varepsilon p^0(T_{res})}{k_B T_{res}} \tag{7.13}$$

The temperature in the flowtube is changing as a known function of time, so if we assume there are no gas losses (to the walls for example) at early times ($T_{res} < T(t)$) the sulfuric acid partial pressure is:

$$p(t) = C_0 k_B T(t) = \frac{\varepsilon p^0(T_{res}) T(t)}{T_{res}} \tag{7.14}$$

This leads to the following expression for the supersaturation as a function of time:

$$S(t) = \frac{p(t)}{p^0(T(t))} = \frac{\varepsilon p^0(T_{res})T(t)}{p^0(T(t))T_{res}} \tag{7.15}$$

For the case when ε = 1, we see this gives the expected $S = 1$ at $T(t) = T_{res}$. In the case where ε < 1, we must solve the following expression for t:

$$\frac{p^0(T(t))}{T(t)} = \frac{\varepsilon p^0(T_{res})}{T_{res}} \tag{7.16}$$

This expression can be solved numerically, and we have used the bisection method to find that $S = S_{crit}$ at between 0.2 and 0.4 s over the full range of T_{res} in the example experiments described here.

7.3 Validation of the simple coagulation model

In forming the simple model presented in sec. 6.2.2, we have made a number of assumptions. In this section we explore the limitations of the model in the context of these assumptions. In modeling coagulation of only 5 sizes, for example, we have assumed that the effect of collisions between particles of larger sizes does not affect the dynamics of sizes 1 through 5 given the timescales and number densities of experimental interest in this system. We have also assumed that the polydispersity of the system can be neglected. We thus count all the particles in mode i as having size i, even though in reality this mode represents a distribution of sizes around the median size.

Comparison of the model against the case of unlimited *m*-mers

In the limit of very long time, this system of equations (eq. 6.16) converges to $n_0/5$ *5-mers*. In reality there is no reason to stop at the *5-mer*; indeed the equilibrium of the physical system would be a single n_0-mer. In order to assure that this choice of model is sufficient to capture the

features of a physical system where all *m*-mers are being formed up to $m = n_0$, we must compare our simplified model to an analytical result which accounts for all possible *m*-mers.

Were we to extend the system of kinetic equations shown in eq. 6.16 up to formation of an n_0-mer, an exact expression for the concentration of a given *m*-mer can be found[3] for the case where the rate constant, *k* does not depend on particle size:

$$n_m(t) = \frac{n_o(t/\tau)^{m-1}}{(1+t/\tau)^{m+1}} \tag{7.17}$$

Here $\tau = 2/kn_0$. For $m = 4$ and $t_c = 4.5$ s, the error is 1% and 10% for $n_0 = 10^7$ and 10^8 cc^{-1} respectively. The error is smaller for all $m < 4$. The ODE system (eq. 6.16) has an advantage over eq. 7.17 as a model for studies on submicron aerosol coagulation since *k* will generally change with size for particles under a micron in diameter.

Comparison of the discrete model against continuous distribution coagulation

The rate of change of a coagulating size distribution of particles can be written as[4]:

$$\frac{\partial n_m(m,t)}{\partial t} = \frac{1}{2}\int_0^m K_{ij}(m_i, m-m_i)n_m(m_i,t)n_m(m-m_i,t)dm_i$$
$$- n_m(m,t)\int_0^\infty K_{ij}(m,m_i)n(m_i,t)dm_i \tag{7.18}$$

Here, $n_m = dN/dm$, so $n(m,t)dm$ is the concentration of particles having masses between *m* and *m+dm* at time *t*. Eq. 7.18 is a so-called *partial integro-differential equation*. The presence of the integral implies much more computational effort than for partial differential equations for example, and pursuit of efficient numerical techniques for such systems is an active area of research[5]. The first term on the right hand side represents the source term building up an infinitesimal mass region of the distribution. The two terms in the first integral reflects that we must sum contributions from all possible collisions resulting in formation of particles of masses within *m* and *m+dm*. As we move to higher *m*, calculation of the integral is more and more

costly. We note that the rate of formation is second order in concentration. The second term is the loss rate (again second order) for the same infinitesimal mass range. Here the integral only needs to account for collisions between particles of mass m and all other sizes (resulting in loss of particles of size m). Although analytical solutions to the general expression (eq. 7.18) are unavailable, an early numerical solution for this system is provided by Drake[6] [1972].

Whereas the simplified model (eq. 6.16) has been shown to reliably deliver number densities for a coagulating system of monodisperse aerosols, we have not validated this model against an analytical result on polydisperse coagulating systems. In the absence of a solution to eq. 7.18, we can approximate the effect of polydisperse coagulation in the following way. Instead of beginning with n_0 particles of size D_1, we begin with n_{1-} of size D_{1-}, n_1 of size D_1 and n_{1+} of size D_{1+}, where particles of sizes 1- and 1+ are very nearly the same size as those of size 1. We can allow the off sizes to be arbitrarily different from size 1 such that the effect of polydispersity can be observed. Keeping track of all the possible collisions of mode-1 particles (1-, 1, and 1+) it can be shown that 5 possible sizes result: 2--, 2-, 2, 2+, and 2++. Here, for example, a particle of size 2++ results from a 1+:1+ collision, whereas a particle of size 2 can come from 1+:1- or a 1:1 collision. In general, for the m^{th} mode, there will be $2m+1$ sizes resulting from collisions of all the different sizes from within mode sizes less than m. Once the possible sizes are constructed, one can describe the dynamics through a system of ordinary differential equations similar to the system in eq. 6.16. For the case of up to $m = 3$ modes, one must write a rate equation for the number densities for each of the 15 different sizes. We constructed such a model whose results we summarize here.

In the case where the coagulation rate constants do not vary with aerosol size, the time variation of the number densities within a given mode of a polydisperse system are identical to those within a discrete system. The particles labeled "1+" or "1-" do not differ from those

labeled "1" with regard to coagulation. This was confirmed with the model. Eq. 6.16 also says nothing about the resulting widths of coagulation modes as a function of the width of mode 1. With the model described above we showed that the mode widths are generally constant (i.e. the initial width of the coagulating system roughly equals that of newly formed modes), showing a slight tendency to decrease with mode. An example from the model output is 1.10, 1.08, and 1.08 for σ_1, σ_2, and σ_3 respectively.

7.4 Conservation of mass in coagulation of discrete sizes

We would like to derive a simple relationship between the initial number density of size 1 particles and the number densities of any other size, *i* at any time, *t*. From mass conservation, the mass of a single particle of size *i* is im_1. The total mass per unit volume of air of all particles of this size is $M_i = n_i m_i$, where n_i is the number density of particle of size *i*. We may therefore write the total mass of the system as, $M = \Sigma M_i = \Sigma n_i m_i$. This must be equal to the mass present initially in the system, $n_0 m_1$, so we have:

$$M = \sum_{i=1}^{\infty} n_i m_i = \sum_{i=1}^{\infty} n_i i m_1 = n_0 m_1$$

such that dividing by m_1 gives:

$$n_0 = \sum_{i=1}^{\infty} i n_i = n_1 + 2n_2 + 3n_3 + \ldots . \qquad (7.19)$$

7.5 Coagulation rate constants

The problem of coagulation has been treated theoretically in multiple texts[7,8,9,10]. In this section, we will summarize the results relevant to this study and suggest a new expression to approximate the coagulation rate through the transition regime.

The coagulation rate constant, k_{ij} for aerosols of size i and j is defined through the rate of collisions between them per volume of air: $z_{ij} = k_{ij} n_i n_j$ where n_i and n_j are the number densities of size i and j particles respectively. Or, as a formal definition for the coagulation rate constant, we have:

$$k_{ij} \equiv \frac{z_{ij}}{n_i n_j} \tag{7.20}$$

As we will see, there is a special case for same-size particle collisions as they reduce their number two-fold per collision. It will be very important that we clearly define the rate constants as we switch back and forth between same-size and different-size collisions.

7.5.1 A general strategy for deriving rate constants

Here, we lay out the method to be used for all subsequent coagulation rate constant derivations. We begin with the collision rate as experienced by one particle. This will generally have the form, $z_i = f(a_i,a_j)n_j$, where z_i is the number of collisions per second felt by a single particle with radii a_i through collisions with particles of radii a_j whose number density is n_j. For unlike particles, we pass trivially to the total number of i:j collisions per unit time per unit volume by multiplying by n_i. So we may write the total collision frequency as $z_{ij} = f(a_i,a_j)n_j n_i$. Once we apply this expression to same-size particles, however, we must be careful to not over-count. In this case a single particle undergoes $z_i = f(a_i)n_i$ collisions per second. If we were to multiply this simply by the number density of such particles, we would count a collision between two particles as two collisions. So for same-size collisions we have: $z_{ii} = \frac{1}{2} f(a_i)n_i^2$ as the total collision frequency. This may seem troublesome as there appears to be a discontinuity in the function z_{ij} as we allow a_i-a_j to become vanishingly small. One can clarify this issue with a simple thought

experiment.[1] We summarize by saying that these formulations of z_{ii} and z_{ij} are entirely self-consistent. The only note of caution is that $z_{ii} = z_{ij} / 2$ when $i = j$.

7.5.2 The kinetic regime

We begin with the simplest case, borrowing concepts from kinetic theory. In this limit we take particle sizes to be much smaller than the apparent mean free path of the particles. This is expected to be applicable for particles for which $a << 20$ nm. In this regime, we may consider the particle motion to be very jagged, much like a molecule. To estimate the collision frequency of a particle with radius a_i with other particles with radii a_j, we imagine a single aerosol sweeping through a collision cylinder with radius a_i+a_j (note: we assume all approaches between aerosols for which the distance between centers is less than a_i+a_j result in a collision). The collision frequency for this single aerosol can now be written as:

$$z = \pi (a_i + a_j)^2 (\bar{c}^2{}_i + \bar{c}^2{}_j)^{1/2} n_j \tag{7.21}$$

The particle mean thermal speed is defined in analogy to gas-phase species:

$$\bar{c}_i = \sqrt{\frac{8 k_B T}{\pi m_i}} \tag{7.22}$$

The term within the square root in eq. 7.21 is the relative speed between colliding particles. If there are n_i such particles per unit volume, then we have a total collision frequency per unit volume given by:

$$z_{ij} = \pi (a_i + a_j)^2 (\bar{c}^2{}_i + \bar{c}^2{}_j)^{1/2} n_i n_j \tag{7.23}$$

For the case of same-size particles, we obtain:

---

[1] *Imagine red particles of size* a_i *colliding with larger blue particles of size* a_j. *There are as many red as blue particles. The collision rate between unlike sizes is given by:* $z_{ij} = f(a_i,a_j)n^2$ *where* $n = n_{red} = n_{blue}$. *Now imagine we shrink the blue particles slowly until* $a_i=a_j$. *The red:blue collision frequency is now given by* $z_{rb}= f(a_i)n^2$. *The total collision frequency is given by summing the red:red, red:blue, and blue:blue collision frequencies. Using* z_{ii} *above, we may write* $z_{rr} = z_{bb} = ½ f(a)n^2$, *and the*

$$z_{ii} = 2\sqrt{2}\pi a^2 \bar{c} n^2 \tag{7.24}$$

Since we have assumed that each collision leads to coagulation, we may use eq. 7.20 and define the coagulation rate constants in this regime:

$$k_{ij} = \pi (a_i + a_j)^2 (\bar{c}^2{}_i + \bar{c}^2{}_j)^{1/2} \quad for \quad i \neq j$$

$$k_{ii} = 2\sqrt{2}\pi a^2 \bar{c} \tag{7.25}$$

These are the coagulation rate constants in the kinetic regime. Our result for k_{ii} is in agreement with Fuchs [1964]. Our result for k_{ij} is in agreement with Friedlander [1977] and Seinfeld [1998], even though they imply it is applicable even when $i=j$. If we extended its validity to this point however, eq. 7.20 would no longer involve a true collision frequency. These authors introduce the factor of ½ later in developing the dynamic equations.

7.5.3 The continuum regime

For particles with radii >> 20 nm, very many molecular collisions must occur before there is a significant change in particle direction. The particle motion in this regime can be considered Brownian. In order to derive an expression for the coagulation rate in the continuum regime, we consider the process starting with Fick's law. This treatment is entirely analogous to the derivation of the diffusion-limited rate constant for reaction in solutions[11]. We first calculate the number of collisions of particles (radius = a_j) with a single particle (radius = a_i) per time. If a steady state concentration gradient has been established (~10^{-5} s for 100 nm particles), the rate at which particles diffuse into an imaginary sphere of radius r surrounding the particle will be constant, given by:

$$\dot{N} = 4\pi r^2 D' \frac{\partial n}{dr} \tag{7.26}$$

---

total collision frequency is thus: $z = z_{rb}+z_{rr}+z_{bb} = 2\ f(a_i)n^2$. If we were to rely solely on z_{ii} above for all the particles, we would say, $z = ½\ f(a_i,)(2n)^2 = 2\ f(a_i)n^2$ which equals the total from adding up the different color combinations.

Upon integration, we impose the boundary condition expressing the concentration far away from the particle as n_j. This leads to:

$$n(r) = \frac{-\dot{N}}{D' 4\pi r} + n_j \tag{7.27}$$

We may further require that $n(a_i+a_j)=0$, since every collision leads to loss at the surface, such that the collision rate experienced by one particle is:

$$z = 4\pi(a_i + a_j)D' n_j \tag{7.28}$$

The assumption that the collisional radius is a_i+a_j allows us to view all other particles as point masses. As before, we may now write the total *i:j* collision rate as:

$$Z_{ij} = 4\pi(a_i + a_j)(D_i + D_j)n_i n_j \tag{7.29}$$

Here *D'* has been recognized as an effective diffusion coefficient between particles diffusing relative to one another, which can be shown to be $D_i + D_j$. From eq. 7.20 above, it follows that coagulation rate constants in the continuum regime are given by:

$$k_{ij} = 4\pi(a_i + a_j)(D_i + D_j) \quad for \quad i \neq j$$

$$k_{ii} = 8\pi a D \tag{7.30}$$

Once again our expression for $k_{ii} = 1/2 * k_{i=j}$ is in agreement with Fuchs. Our result for k_{ij} is in agreement with Friedlander, Seinfeld and Pruppacher, even though they imply it is applicable even when *i=j*. Our choice to write the coagulation rate constants this way reflects our adherence to using eq. 7.20 as a global working definition. This will make writing the dynamic equations more intuitive since we have only to keep up with the collision rates for each size.

7.5.4 The transition regime

For most coagulation of atmospheric relevance (as well as for this study), radii typically span 10 to 1000 nm, and neither the kinetic nor the continuum regime is fully applicable. Rate constants

in this transition regime have been derived by Fuchs[7]. Here we will propose a much simpler approximation of the transition regime than that given in the literature.

We may physically imagine the coagulation process to consist of two components; one kinetic, the other continuous. It is therefore reasonable that we should be able to model the transition regime by mixing the two expressions valid in each regime. The simplest way of mathematically mixing the two rate constants such that one recovers the prescribed limits is given by the following:

$$K_{trans} = \frac{K_{kin} K_{cont}}{K_{kin} + K_{cont}} \tag{7.31}$$

This simplified expression is plotted against the more rigorous (and much more complex) expression provided by Fuchs (and formulated by Seinfeld) for like-size collisions in fig. 7-4.

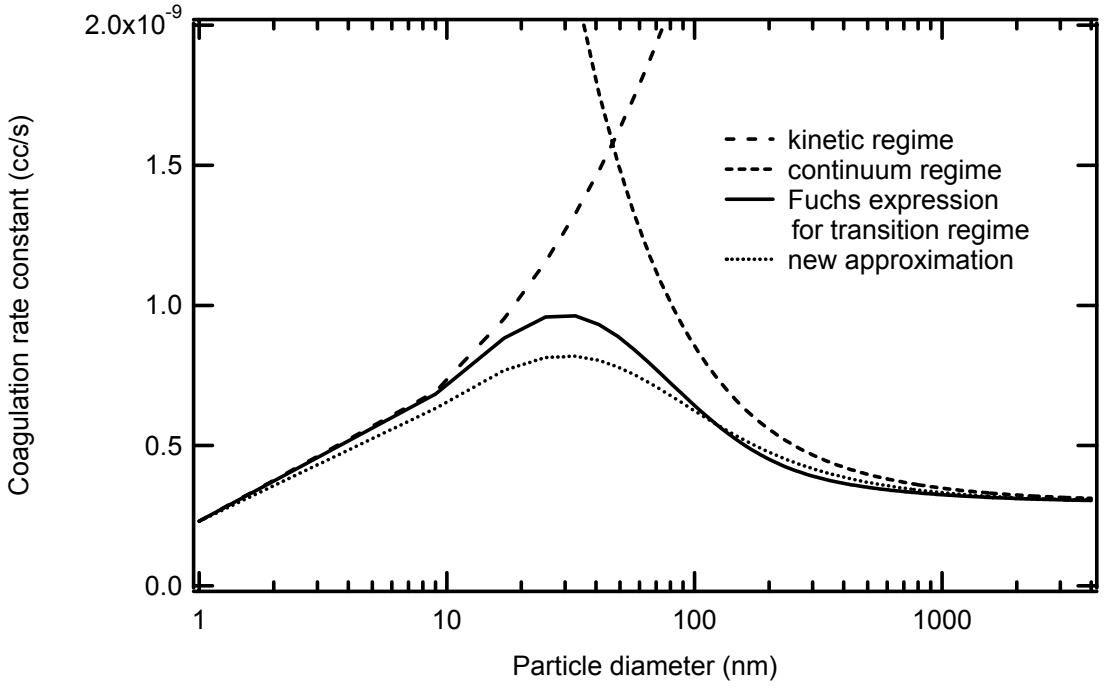

Figure 7-4: The approximation presented here (7.31) compared to the Fuchs expression of the coagulation rate constant for the transition regime.

As is evident in fig. 7-1, the new approximation presented here is in good agreement with the more complicated expression derived by Fuchs. As can be seen in the functional form of eq. 7.31, the bridge for the transition regime was built from the limiting regimes in a resistor-like fashion. The proximity of the approximation to the Fuchs result can be taken as an indicator of the extent to which both continuum and kinetic mechanisms are acting independently (uncoupled) during physical coagulation of aerosol particles.

Chapter 7 Appendix

[1] J. Seinfeld and H. Pandis, *Atmospheric Chemistry and Physics*, (Wiley, 1998, 568).

[2] Seinfeld and Pandis, p. 597.

[3] Friedlander, *Smoke, Dust, and Haze*, (Wiley, 1977, 181).

[4] Fuchs, *The Mechanics of Aerosols*, (Dover, 1964, 299).

[5] D. D. Obrigkeit, *Numerical Solutions of Multicomponent Population Balance Systems with Applications to Particulate Processes*, PhD Thesis, MIT, 2001.

[6] R. L. Drake, *Topics in Current Aerosol Research*, (Pergamon, New York, 1972).

[7] Seinfeld and Pandis, p. 656.

[8] Fuchs, p. 288.

[9] Friedlander, p. 175.

[10] Pruppacher and Klett, *Microphysics of Clouds and Precipitaion*, (Kluwer, 1997, 454).

[11] Steinfeld, Francisco, and Hase, *Chemical Kinetics and Dynamics*, (Prentice Hall, 1999, 129).